Performance Analysis of NOMA-Based Symbiotic Ambient Backscatter Communication

Xinying Li, Lijun Zhang

***Abstract*—Non-orthogonal multiple access (NOMA) and ambient backscatter communication (AmBC) are promising technologies to enable spectrum efficiency in wireless communication systems. In this paper, we propose a downlink NOMA multiplexing-based Symbiotic radio (SR) AmBC system over Rayleigh fading channels. The system consists of one source node S, one backscatter device (BD), one nearby cellular user (User 1), and one far-away cellular user (User 2). In light of a viable non-linear energy harvesting (EH) model, we implement the most effective dynamic reflection strategy to enhance the backscattered signal's power, adhering to the BD's energy-causality limitations. The analytical expressions for the outage probability of the proposed system are derived. Moreover, we compared the performance of the NOMA-based system against the OMA-based system. Simulation results verified our derived expressions and showed that the consumed power by the BD had a remarkable influence on the system outage performance.**

***Index Terms*—Non-orthogonal multiple access (NOMA); symbiotic radio (SR); ambient backscatter communication(AmBC); nonlinear energy harvesting (EH); outage probability**

I. Introduction

Non-orthogonal multiple access (NOMA) technology is considered as an effective technology that scales up massive access and improves spectrum resources [1]. It is different from traditional orthogonal multiple access (OMA) technology, where the signals of different users are orthogonal to each other to avoid mutual interference. Non-orthogonal multiple access allows multiple users to communicate on the same orthogonal resource block, which can effectively improve the spectrum utilization rate and increase the throughput of users at the edge of the cell [2]. To achieve non-orthogonal multiple access, superposition coding is employed at the transmitter side, while successive interference cancellation (SIC) is utilized at the receiver side [3]. Regarded as a technology with great potential, Ambient Backscatter Communication (AmBC) has been celebrated for its ability to enable communication that is both low-power and efficient in energy use, marking it as an innovative solution for sustainable wireless networks [4]. Combining NOMA with AmBC helps solve the problem of limited energy and spectrum resources in Internet-of-Things (IoT).

Manuscript received September 28, 2023; revised April 16, 2024. This work was supported by Science and Technology Planning Project of Gansu (22JR5RA361,23JRRA894), Key research and development Planning Project of Gansu Province (23YFWA0007).

Xinying Li is an associate professor at School of Electronic and Information Engineering, Lanzhou Jiaotong University, Lanzhou 730070, China. (Corresponding author to provide e-mail: 874260442@qq.com).

Lijun Zhang is a postgraduate student at School of Electronic and Information Engineering, Lanzhou Jiaotong University, Lanzhou 730070, China. (e-mail: 2941471138@qq.com).

Within the AmBC system, the backscatter device (BD) conveys its communication by altering the radio frequency (RF) source signals derived from legacy signals, such as cellular or WiFi. It then redirects these altered signals towards the designated receiver. Concurrently, it extracts energy from legacy signals to offset the energy consumption of its circuitry [5]. The BD does not require active devices; for example, oscillators and analog-to-digital/digital-to-analog converters. This results in a great reduction in energy consumption [6]. Symbiotic radio (SR) is introduced into the backscattering communication system so that the ambient signal and the backscattering signal have a common target receiver. The SIC technique can be used in the demodulation of backscattered signals to eliminate the interference caused by strong ambient signals [7].

Based on the above discussion, a combination of AmBC or SR with NOMA could boost the performance of energy and spectrum efficiency. To improve the system outage performance, previous researchers [8] proposed a tag selection scheme for the BackCom system with multiple tags to maximize the received SNR at the destination being selected for transmission. In another study [9], the authors analyzed a wireless-powered backscatter communication system to enhance the system performance in terms of outage probability and throughput. Further research [10] have examined a tag selection strategy aimed at bolstering secure transmission within a passive backscatter communication system, involving numerous tags and a single eavesdropper. The analysis took into account the power utilization of the tags and implemented an optimal dynamic reflection coefficient (RC) to amplify the power of the backscattered signals. In other work [11], the performance evaluation was investigated for a dynamic NOMA-BackCom scheme, characterized by an adaptive approach to multiplexing backscatter nodes and selecting the reflection coefficient variably. In another study [12], the outage probabilities (OPs) were investigated for NOMA-based SR-AmBC systems under Nakagami-m fading channels. Other authors [13] derived the expressions of the outage probabilities and the ergodic rates for both backscatter-NOMA and SR systems with fixed RC. Other research [14] investigated the outage probability and ergodic rate for a cognitive radio (CR)-enabled AmBC system with NOMA functionality. In previous research [15], the ergodic capacity (EC) was investigated for a downlink NOMA-based SR-AmBC system under Nakagami-m fading channels. Other authors [16] proposed a cognitive AmBC NOMA model to strengthen spectrum efficiency and analyzed the outage probability and ergodic rate. Other research [17] have examined a symbiotic backscatter-NOMA

system, wherein the backscatter communication operates in tandem with the principal NOMA signal. This is achieved by modulating the reflection coefficient at the BD, from which the connection outage probability (COP) has been deduced.

In most studies combining NOMA and AmBC, a fixed RC design is used for performance analysis. The default BD circuit power consumption has a small impact on the system, and the BD loss is often ignored on the system [11]- [17]. Therefore, it is worth analyzing the performance of the system considering the consumption of the BD itself. Therefore, different from previous studies, we analyze the outage performance of the system as a whole.

The main contributions of this paper can be summarized as follows:

1) It presents analytical expressions for outage probabilities, premised on the assumption that wireless channels exhibit Rayleigh fading and include additive white Gaussian noise (AWGN).

2) In contrast to static RC configurations, this study introduces an adaptive dynamic RC strategy that optimizes the strength of reflected signals in accordance with the BD circuit's power requirements.

3) Through empirical evidence, the research corroborates the theoretical propositions and demonstrates the enhanced efficacy of the backscatter-NOMA system over traditional OMA approaches.

II. System Model

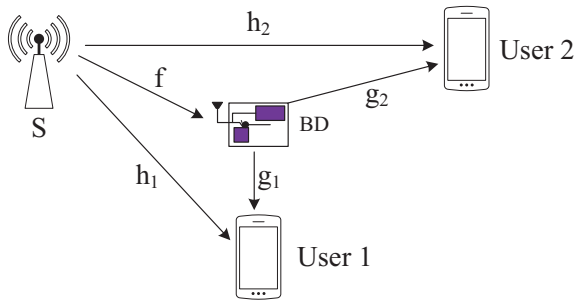

Fig. 1. Downlink NOMA-based SR-AmBC system model.

In this study, we examine the downlink NOMA-based SR AmBC system illustrated in Fig. 1, which includes one source node S, one BD, one nearby cellular user named User1, and one far-away cellular user named User2. A single antenna is equipped on each node. The channel coefficients of the links, that is, S→User 1, S→User 2, S→BD, BD→User 1 and BD→User 2, are denoted by h_1, h_2, h_3, h_4 and h_5, respectively. All channel coefficients are assumed to follow the Rayleigh fading under AWGN noise. The channel gains are denoted by $|h_1|^2$, $|h_2|^2$, $|h_3|^2$, $|h_4|^2$ and $|h_5|^2$, which follow an exponential distribution with means of $\frac{1}{\lambda_1}$, $\frac{1}{\lambda_2}$, $\frac{1}{\lambda_3}$, $\frac{1}{\lambda_4}$ and $\frac{1}{\lambda_5}$, respectively. The transmitted power from S conveys its multiplexed messages as well as supports the BD transmission. It is assumed that S adopts NOMA for multiplexing two messages, x_1 and x_2, which are intended for User 1 and User 2.

The transmitted message at the S can be written as

$$x_s = \sqrt{a_1 P_s} x_1 + \sqrt{a_2 P_s} x_2. \tag{1}$$

Here, x_1 and x_2 are the messages with unit power transmitted to User 1 and User 2, respectively; and P_s is the total transmit power of the S with power allocation factors a_1 and a_2 to x_1 and x_2, respectively. It can be assumed that $a_1 < a_2$ and $a_1 + a_2 = 1$.

A. Received Signal at User 1

The received signal at User 1 can be written as

$$y_1 = h_1 x_s + \sqrt{\eta\beta^*} f g_1 x_s x_t + n_1, \tag{2}$$

where x_t is the backscattered signal by the BD, β^* is RC, and n_1 is the received additive white Gaussian noise with zero mean and variance σ^2.

The signal to interference plus noise ratio (SINR) and signal-to-noise ratio (SNR) are given below with the assumption of perfect channel state information (CSI). User 1 decodes x_2, followed by x_1, and finally x_t with the SIC technique. When decoding x_2, the received SINR is given as

$$\gamma_{1,2} = \frac{a_2 \rho |h_1|^2}{a_1 \rho |h_1|^2 + \eta\beta^* \rho |f|^2 |g_1|^2 + 1}, \tag{3}$$

where $\rho = \frac{P_s}{\delta^2}$ denotes the transmitted SNR, and η is the energy conversion efficiency.

When User 1 decodes x_2 successfully, it can be culled from y_1. User 1 can then decode its own message x_1. When decoding x_1, the received SINR is given as

$$\gamma_{1,1} = \frac{a_1 \rho |h_1|^2}{\eta\beta^* \rho |f|^2 |g_1|^2 + 1}. \tag{4}$$

Using a perfect SIC technique, User 1 can decode the backscattered message of BD x_t. The received SINR at User 1 to detect x_t is given as

$$\gamma_{1,t} = \eta\beta^* \rho |f|^2 |g_1|^2. \tag{5}$$

B. Received Signal at User 2

The received signal at User 1 can be written as

$$y_2 = h_2 x_s + \sqrt{\eta\beta^*} f g_2 x_s x_t + n_2, \tag{6}$$

where n_2 is the received additive white Gaussian noise at User 2 with zero mean and variance σ^2.

User 2 only needs to decode its own message x_2 by treating other signal components as interference. Then, the received SINR at User 2 to detect x_2 can be given as

$$\gamma_{2,2} = \frac{a_2 \rho |h_2|^2}{a_1 \rho |h_2|^2 + \eta\beta^* \rho |f|^2 |g_2|^2 + 1}. \tag{7}$$

A practical non-linear energy harvesting (EH) model [9] can be used to describe the harvested power P_0 at the BD. Particularly, P_0 can be expressed as

$$P_0 = \frac{P_{\max}(1 - \exp(-v_1 P_r + v_1 v_0))}{1 + \exp(-v_1 P_r + v_1 v_2)}, \tag{8}$$

where $P_{\max}$ is the maximum harvestable power when the circuit is saturated; P_r is the input power for energy harvesting (EH) at BD, that is, $P_r = (1-\beta^*)P_s|h_3|^2$; v_0 denotes the sensitivity threshold; and v_1 and v_2 are fixed parameters determined by the resistance, capacitance, and diode turn-on voltage.

Let P_c denote the circuit power consumption at the BD. The BD has enough energy for the circuit operation when $P_0 \geq P_c$. Considering the fact that $0 \leq \beta \leq 1$, the optimal dynamic RC can be obtained when $P_0 = P_c$. Moreover, β^* can be written as

$$\beta^* = \max(1 - \frac{\Phi}{P_s|h_3|^2}, 0), \tag{9}$$

where $\Phi = \frac{\log \frac{P_{\max} e^{v_1 v_2} + P_c e^{v_1 v_0}}{P_{\max} - P_c}}{v_1}$. By recalling the derivation of β^*, it is easy to find that as long as $\beta^* > 0$ then BD can reflect the signal; and $\beta^* = 0$ means that the BD keeps silent and the backscatter link is in outage.

When the entire reflection link is interrupted, the received signal at User 1 can be written as

$$y_{D1} = h_1 x_s + n_1. \tag{10}$$

The SINR at User 1 to detect x_2 can be given as

$$\gamma_{D1,2} = \frac{a_2 \rho |h_1|^2}{a_1 \rho |h_1|^2 + 1}. \tag{11}$$

The SINR at User 1 to detect x_1 can be given as

$$\gamma_{D1,1} = a_1 \rho |h_1|^2. \tag{12}$$

The received signal at User 2 can be given as

$$y_{D2} = h_2 x_s + n_2. \tag{13}$$

The SINR at User 2 to detect x_2 can be given as

$$\gamma_{D2,2} = \frac{a_2 \rho |h_2|^2}{a_1 \rho |h_2|^2 + 1}. \tag{14}$$

III. Performance Analysis

This section analyzes the outage performance for the considered backscatter-NOMA system. The exact closed-form expressions of the outage probabilities are derived in the following subsections.

A. Outage Probability of User 2

The outage event of User 2 occurs if User 2 cannot decode x_2, where τ_2 is threshold value, $\tau_2 = 2^{R_{\text{th2}}} - 1$, and R_{th2} is the target data rate for User 2. Then, the outage probability for User 2 can be written as

$$OP_2 = \underbrace{\Pr(\gamma_{D2,2} < \tau_2, \beta^* = 0)}_{A_1} + \underbrace{\Pr(\gamma_{2,2} < \tau_2, \beta^* > 0)}_{A_2}. \tag{15}$$

Let $X = |h_1|^2$, $Y = |h_2|^2$, $Z = |h_3|^2$, $V = |h_4|^2$ and $W = |h_5|^2$ in the following. Then, the probability density functions of X, Y, Z, V, and W are $f(x) = \lambda_1 e^{-\lambda_1 x}$, $f(y) = \lambda_2 e^{-\lambda_2 y}$, $f(z) = \lambda_3 e^{-\lambda_3 z}$, $f(v) = \lambda_4 e^{-\lambda_4 v}$, and $f(w) = \lambda_5 e^{-\lambda_5 w}$, respectively.

$$\begin{aligned} A_1 &= \Pr\left(|h_2|^2 < \frac{\tau_2}{\rho t}, |f|^2 < \frac{\Phi}{P_s}\right) \\ &= \left(1 - e^{-\frac{\lambda_2 \tau_2}{\rho t}}\right)\left(1 - e^{-\frac{\lambda_3 \Phi}{P_s}}\right). \end{aligned} \tag{16}$$

A_2 can be derived as given in (17).

Here, $u = z - \frac{\Phi}{P_s}$ through proper simplification and by using the integration $\int_0^\infty \frac{e^{-\mu x}}{x+\beta} dx = -e^{\beta\mu}\text{Ei}(-\mu\beta)$.

$$\begin{aligned} A_2 &= \Pr\left(|h_2|^2 < \frac{\eta\beta^*|f|^2|g_2|^2\tau_2}{t} + \frac{\tau_2}{\rho t}, \beta^* > 0\right) \\ &= \Pr\left(y < \frac{\eta\tau_2 w\left(z - \frac{\Phi}{P_s}\right)}{t} + \frac{\tau_2}{\rho t}, z > \frac{\Phi}{P_s}\right) \\ &= e^{-\frac{\lambda_3\Phi}{P_s}} - \lambda_3\lambda_5 e^{-\frac{\lambda_2\tau_2}{\rho t}} e^{-\frac{\lambda_3\Phi}{P_s}} \int_0^\infty \frac{t e^{-\lambda_5 w}}{\eta\lambda_2\tau_2 w + \lambda_3 t} dw \\ &= e^{-\frac{\lambda_3\Phi}{P_s}} + \lambda_3\lambda_5 e^{-\frac{\lambda_2\tau_2}{\rho t}} e^{-\frac{\lambda_3\Phi}{P_s}} \frac{t}{\eta\lambda_2\tau_2} e^{\frac{\lambda_3\lambda_5 t}{\eta\lambda_2\tau_2}} Ei\left(-\frac{\lambda_3\lambda_5 \text{t}}{\eta\lambda_2\tau_2}\right). \end{aligned} \tag{17}$$

By combining (16) and (17), the closed-form analytical result for the outage probability of User 2 can be expressed as

$$OP_2 = \begin{cases} A_1 + A_2, & otherwise; \\ 1, & \frac{a_2}{\tau_2} < a_1 \leq 1. \end{cases} \tag{18}$$

B. Outage Probability of User 1

When User 1 fails to decode message x_1 or x_2, an outage event occurs, where τ_1 is a threshold value, $\tau_1 = 2^{R_{\text{th1}}} - 1$, and R_{th1} is the target data rate for User 1. Therefore, the outage probability of User 1 decoding x_1 can be written as

$$\begin{aligned} OP_1 = 1 &- \underbrace{\Pr\left(\gamma_{D1,2} \geq \tau_2, \gamma_{D1,1} \geq \tau_1, \beta^* = 0\right)}_{B_1} \\ &- \underbrace{\Pr\left(\gamma_{1,2} \geq \tau_2, \gamma_{1,1} \geq \tau_1, \beta^* > 0\right)}_{B_2}, \end{aligned} \tag{19}$$

where B_1 can be derived as given below.

$$\begin{aligned} B_1 &= \Pr\left(|h_1|^2 \geq \frac{\tau_2}{\rho t}, |h_1|^2 \geq \frac{\tau_1}{\rho a_1}, |f|^2 < \frac{\Phi}{P_s}\right) \\ &= \begin{cases} (1) = \Pr\left(|h_1|^2 \geq \frac{\tau_1}{\rho a_1}, |f|^2 < \frac{\Phi}{P_s}\right) \\ \quad = e^{-\frac{\lambda_1\tau_1}{\rho a_1}}\left(1 - e^{-\frac{\lambda_3\Phi}{P_s}}\right), \quad 0 < a_1 \leq \frac{a_2\tau_1}{\tau_2(1+\tau_1)}; \\ (2) = \Pr\left(|h_1|^2 \geq \frac{\tau_2}{\rho t}, |f|^2 < \frac{\Phi}{P_s}\right) \\ \quad = e^{-\frac{\lambda_1\tau_2}{\rho t}}\left(1 - e^{-\frac{\lambda_3\Phi}{P_s}}\right), \quad \frac{a_2\tau_1}{\tau_2(1+\tau_1)} < a_1 \leq \frac{a_2}{\tau_2}, \end{cases} \end{aligned} \tag{20}$$

where $t = a_2 - a_1\tau_2$. Moreover, B_2 can be derived through (21).

$$B_2 = \Pr\left(|\mathrm{h}_1|^2 \geq \frac{\eta|g_1|^2\left(|f|^2-\frac{\Phi}{P_s}\right)\tau_2}{t}+\frac{\tau_2}{\rho t}, |\mathrm{h}_1|^2 \geq \frac{\eta|g_1|^2\left(|f|^2-\frac{\Phi}{P_s}\right)\tau_1}{a_1}+\frac{\tau_1}{\rho a_1}, |f|^2 > \frac{\Phi}{P_s}\right)$$
$$= \begin{cases} (3) = \Pr\left(|\mathrm{h}_1|^2 \geq \frac{\eta|g_1|^2\left(|f|^2-\frac{\Phi}{P_s}\right)\tau_1}{a_1}+\frac{\tau_1}{\rho a_1}, |f|^2 > \frac{\Phi}{P_s}\right), \ 0 < a_1 \leq \frac{a_2\tau_1}{\tau_2(1+\tau_1)}; \\ (4) = \Pr\left(|\mathrm{h}_1|^2 \geq \frac{\eta|g_1|^2\left(|f|^2-\frac{\Phi}{P_s}\right)\tau_2}{t}+\frac{\tau_2}{\rho t}, |f|^2 > \frac{\Phi}{P_s}\right), \ \frac{a_2\tau_1}{\tau_2(1+\tau_1)} < a_1 \leq \frac{a_2}{\tau_2}; \end{cases} \quad (21)$$

When $t \leq 0$, then $\frac{a_2}{\tau_2} < a_1 \leq 1$, $B_1 = 0$ and $B_2 = 0$.

$$\begin{aligned}(3) &= \Pr\left(x \geq \frac{\eta v\left(z-\frac{\Phi}{P_s}\right)\tau_1}{a_1}+\frac{\tau_1}{\rho a_1}, z > \frac{\Phi}{P_s}\right) \\ &= \int_0^\infty \int_{\frac{\Phi}{P_s}}^\infty e^{-\frac{\lambda_1\tau_1}{\rho a_1}} e^{-\frac{\lambda_1\eta\tau_1 v\left(z-\frac{\Phi}{P_s}\right)}{a_1}} \lambda_3\lambda_4 e^{-\lambda_3 z} e^{-\lambda_4 v} dz dv \\ &= \lambda_3\lambda_4 e^{-\frac{\lambda_1\tau_1}{\rho a_1}} e^{-\frac{\lambda_3\Phi}{P_s}} \int_0^\infty \frac{a_1 e^{-\lambda_3 u}}{\lambda_1\eta\tau_1 u + a_1\lambda_4} du \\ &= -\lambda_3\lambda_4 e^{-\frac{\lambda_1\tau_1}{\rho a_1}} e^{-\frac{\lambda_3\Phi}{P_s}} \frac{a_1}{\lambda_1\eta\tau_1} e^{\frac{\lambda_3\lambda_4 a_1}{\lambda_1\eta\tau_1}} Ei\left(-\frac{\lambda_3\lambda_4 a_1}{\lambda_1\eta\tau_1}\right).\end{aligned} \quad (22)$$

$$\begin{aligned}(4) &= \Pr\left(x \geq \frac{\eta v\left(z-\frac{\Phi}{P_s}\right)\tau_2}{t}+\frac{\tau_2}{\rho t}, z > \frac{\Phi}{P_s}\right) \\ &= \int_0^\infty \int_{\frac{\Phi}{P_s}}^\infty e^{-\frac{\lambda_1\tau_2}{\rho t}} e^{-\frac{\lambda_1\eta\tau_1 v\left(z-\frac{\Phi}{P_s}\right)}{t}} \lambda_3\lambda_4 e^{-\lambda_3 z} e^{-\lambda_4 v} dz dv \\ &= \lambda_3\lambda_4 e^{-\frac{\lambda_1\tau_2}{\rho t}} e^{-\frac{\lambda_3\Phi}{P_s}} \int_0^\infty \int_0^\infty e^{-\frac{\lambda_1\eta\tau_2 vu}{t}} e^{-\lambda_3 u} e^{-\lambda_4 v} du dv \\ &= \lambda_3\lambda_4 e^{-\frac{\lambda_1\tau_1}{\rho t}} e^{-\frac{\lambda_3\Phi}{P_s}} \int_0^\infty \frac{t e^{-\lambda_3 u}}{\lambda_1\eta\tau_2 u + t\lambda_4} du \\ &= -\lambda_3\lambda_4 e^{-\frac{\lambda_1\tau_1}{\rho t}} e^{-\frac{\lambda_3\Phi}{P_s}} \frac{t}{\lambda_1\eta\tau_2} e^{\frac{\lambda_3\lambda_4 t}{\lambda_1\eta\tau_2}} Ei\left(-\frac{\lambda_3\lambda_4 t}{\lambda_1\eta\tau_2}\right).\end{aligned} \quad (23)$$

Combining all the derived results, the closed-form analytical result for the outage probability of User 1 decoding x_1 can be expressed as

$$OP_1 = \begin{cases} 1-(1)-(3), & 0 < a_1 \leq \frac{a_2\tau_1}{\tau_2(1+\tau_1)}; \\ 1-(2)-(4), & \frac{a_2\tau_1}{\tau_2(1+\tau_1)} < a_1 \leq \frac{a_2}{\tau_2}; \\ 1, & \frac{a_2}{\tau_2} < a_1 \leq 1, a_1 = 0; \end{cases} \quad (24)$$

where $a_1 = 0$. All the transmission power is allocated to User 2; hence, an outage event occurs for User 1.

C. Outage Probability of the BD

Since x_t is the weakest message, the receiver must use SIC to decode message x_2 and x_1 to decode x_t, and thus the BD outage occurs when the system fails to decode any of the three messages. The SINR threshold at BD for detecting x_t is τ_3.

Therefore, the corresponding outage probability for BD can be written as

$$\begin{aligned}OP_{BD} &= 1 - \Pr\left(\gamma_{1,2} \geq \tau_2, \gamma_{1,1} \geq \tau_1, \gamma_{1,t} \geq \tau_3, \beta^* > 0\right) \\ &= 1 - \underbrace{\Pr\left(\gamma_{1,2} \geq \tau_2, \gamma_{1,1} \geq \tau_1, \beta^* > 0\right)}_{B_2} \\ &\times \underbrace{\Pr\left(\gamma_{1,t} \geq \tau_3, \beta^* > 0\right)}_{C_1}.\end{aligned} \quad (25)$$

In (25), the corresponding outage probability C_1 can be written as

$$\begin{aligned}C_1 &= \Pr\left(v \geq \frac{\tau_3}{\eta\rho\left(z-\frac{\Phi}{P_s}\right)}, z > \frac{\Phi}{P_s}\right) \\ &= \int_{\frac{\Phi}{P_s}}^\infty e^{-\frac{\lambda_4\tau_3}{\eta\rho\left(z-\frac{\Phi}{P_s}\right)}} \lambda_3 e^{-\lambda_3 z} dz \\ &= \lambda_3 e^{-\frac{\lambda_3\Phi}{P_s}} \int_0^\infty e^{-\frac{\lambda_4\tau_3}{\eta\rho u}-\lambda_3 u} du \\ &= e^{-\frac{\lambda_3\Phi}{P_s}} \sqrt{\frac{4\lambda_3\lambda_4\tau_3}{\eta\rho}} K_1\left(\sqrt{\frac{4\lambda_3\lambda_4\tau_3}{\eta\rho}}\right).\end{aligned} \quad (26)$$

$K_1(\cdot)$ is the first order modified Bessel function of the second kind through proper simplification and by using the integration $\int_0^\infty e^{-\frac{\beta}{4x}-\gamma x} dx = \sqrt{\frac{\beta}{\gamma}} K_1\left(\sqrt{\beta\gamma}\right)$.

By combining all the derived results, the final closed-form analytical result for the outage probability of BD can be expressed as given below.

$$OP_{BD} = \begin{cases} 1-(3)\times C_1, & 0 < a_1 \leq \frac{a_2\tau_1}{\tau_2(1+\tau_1)}; \\ 1-(4)\times C_1, & \frac{a_2\tau_1}{\tau_2(1+\tau_1)} < a_1 \leq \frac{a_2}{\tau_2}; \\ 1, & \frac{a_2}{\tau_2} < a_1 \leq 1, a_1 = 0; \end{cases} \quad (27)$$

D. Overall Outage Probability

Considering the system is a whole, if any path transmission is not successful, then the whole system is considered to have

failed. Therefore, the overall outage probability can be written as

$$\begin{aligned} OP_{all} &= 1 - \Pr\left(\gamma_{2,2} \geq \tau_2, \gamma_{1,2} \geq \tau_2, \gamma_{1,1} \geq \tau_1, \gamma_{1,t} \geq \tau_3, \beta^* > 0\right) \\ &\quad - \Pr\left(\gamma_{D2,2} \geq \tau_2, \gamma_{D1,2} \geq \tau_2, \gamma_{D1,1} \geq \tau_1, \beta^* = 0\right) \\ &= 1 - \underbrace{\Pr\left(\gamma_{2,2} \geq \tau_2, \beta^* > 0\right)}_{P_2} \\ &\quad \times \underbrace{\Pr\left(\gamma_{1,2} \geq \tau_2, \gamma_{1,1} \geq \tau_1, \beta^* > 0\right)}_{B_2} \times \underbrace{\Pr\left(\gamma_{1,t} \geq \tau_3, \beta^* > 0\right)}_{C_1} \\ &\quad - \underbrace{\Pr\left(\gamma_{D2,2} \geq \tau_2, \beta^* = 0\right)}_{P_1} \\ &\quad \times \underbrace{\Pr\left(\gamma_{D1,2} \geq \tau_2, \gamma_{D1,1} \geq \tau_1, \beta^* = 0\right)}_{B_1}. \end{aligned} \tag{28}$$

In (28), the corresponding outage probabilities P_1 and P_2 can be written as

$$\begin{aligned} P_2 &= \Pr\left(|h_2|^2 > \frac{\eta\beta^*|f|^2|g_2|^2\tau_2}{t} + \frac{\tau_2}{\rho t}, \beta^* > 0\right) \\ &= \Pr\left(y > \frac{\eta\tau_2 w\left(z - \frac{\Phi}{P_s}\right)}{t} + \frac{\tau_2}{\rho t}, z > \frac{\Phi}{P_s}\right) \\ &= \int_0^{\infty}\int_{\frac{\Phi}{P_s}}^{\infty} e^{-\frac{\lambda_2\tau_2}{\rho t}} e^{-\frac{\lambda_2\eta\tau_2 w\left(z-\frac{\Phi}{P_s}\right)}{t}} \lambda_3\lambda_5 e^{-\lambda_3 z} e^{-\lambda_5 w} dz dw \\ &= \lambda_3\lambda_5 e^{-\frac{\lambda_2\tau_2}{\rho t}} e^{-\frac{\lambda_3\Phi}{P_s}} \int_0^{\infty} \frac{t e^{-\lambda_5 w}}{\eta\lambda_2\tau_2 w + \lambda_3 w} dw \\ &= -\lambda_3\lambda_5 e^{-\frac{\lambda_2\tau_2}{\rho t}} e^{-\frac{\lambda_3\Phi}{P_s}} \frac{t}{\eta\lambda_2\tau_2} e^{\frac{\lambda_3\lambda_5 t}{\eta\lambda_2\tau_2}} Ei\left(-\frac{\lambda_3\lambda_5 t}{\eta\lambda_2\tau_2}\right). \end{aligned} \tag{29}$$

$$\begin{aligned} P_1 &= \Pr\left(|h_2|^2 > \frac{\tau_2}{\rho t}, |f|^2 < \frac{\Phi}{P_s}\right) \\ &= e^{-\frac{\lambda_2\tau_2}{\rho t}}\left(1 - e^{-\frac{\lambda_3\Phi}{P_s}}\right). \end{aligned} \tag{30}$$

By combining all the derived results, the final closed-form analytical result for the outage probability of overall can be expressed as given below.

$$OP_{all} = \begin{cases} 1 - P_2 \times (3) \times C_1 - P_1 \times (1), & 0 < a_1 \leq \dfrac{a_2\tau_1}{\tau_2(1+\tau_1)}; \\ 1 - P_2 \times (4) \times C_1 - P_1 \times (2), & \dfrac{a_2\tau_1}{\tau_2(1+\tau_1)} < a_1 \leq \dfrac{a_2}{\tau_2}; \\ 1, & \dfrac{a_2}{\tau_2} < a_1 \leq 1, a_1 = 0; \end{cases} \tag{31}$$

To gain deeper insights, it is possible to examine the achievable diversity order of the system outage probability by considering the high SNR regime. Based on analytical result, the diversity order of the proposed model can be derived as

$$D_i = -\lim_{\rho\to\infty} \frac{\log OP_i^{\infty}}{\log \rho} = 0, \tag{32}$$

where $i = 1, 2, BD, all$. When ρ goes to infinity, the outage probability becomes a constant.

IV. Numerical Results

In the simulations, the parameters for the non-linear EH model were set as follows [9]: $P_{max} = 240$ μW, $v_0 = 5$ μW, $v_1 = 5000$, $v_2 = 0.0002$, and $P_c = 8.9$ μW. The parameters were assumed as follows: $\sigma^2 = -30$ dBm, $\eta = 0.6$, $\lambda_1 = 0.4$, $\lambda_2 = 5$, $\lambda_3 = 5$, $\lambda_4 = 10$, $\lambda_5 = 10$, $\tau_1 = 1$, $\tau_2 = 1$, $\tau_3 = 0.1$,

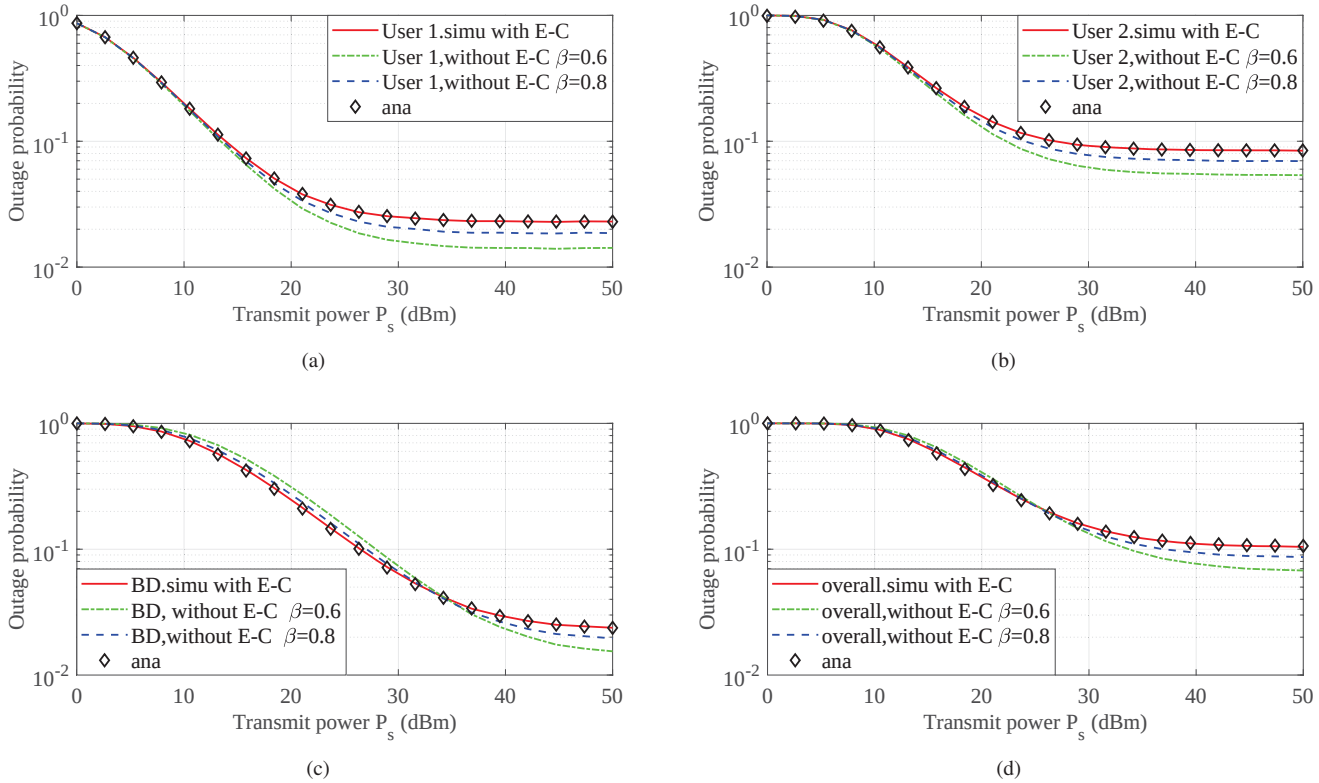

Fig. 2. The Outage performance of proposed system with the dynamic RC.

$a_1 = 0.2$ and $a_2 = 0.8$. In the following, "ana" is denoted as the analytical result, and "simu" is the simulation result.

In Fig. 2, 'with E-C' considers the energy constraint condition and 'without E-C' is without, indicating that regardless of the fixed RC value, the system disregards the harvested power in meeting the BD's needs. It can be observed that the outage probability of 'with E-C' is higher than 'without E-C' for OP_1 and OP_2 with any fixed RC $\beta = 0.6$ or $\beta = 0.8$. Additionally, the OP_{BD} and OP_{all} in 'with E-C' is better than that of 'without E-C' up to certain power. Therefore, the consumed power by the BD has a remarkable influence on the system outage performance. The outage performance of the system is overestimated without considering BD consumption. Thus, the consumed power by the BD should be considered when analyzing the performance of the BackCom system.

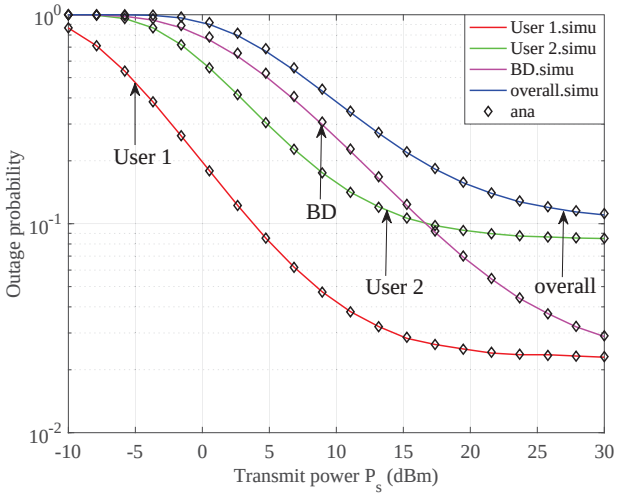

Fig. 3. The Outage performance of proposed system.

As shown in Fig. 3, the analytical results and the simulation results perfectly match the simulation results when the outage probability curves remained unchanged in the high P_s regime. Moreover, the overall outage probability considered all the conditions. If any condition was not up to standard, then the whole system was considered to be an unsuccessful transmission, and thus the outage probability was the highest compared with each user.

To evaluate the performance of the proposed system in this paper, Fig. 4 compares the performance of the the backscatter-NOMA scheme with the OMA scheme. As shown, the outage probability based on the NOMA system is lower. This is because NOMA can transmit information to User 1 and User 2 at the same time. Compared with the OMA scheme, the transmission time of the NOMA scheme is doubled, and the threshold SNR is reduced by 1/2 when the target rate remains the same, which ultimately leads to a lower outage probability. Therefore, the backscatter-NOMA scheme outperforms the OMA scheme in terms of the outage probability.

Figure 5 shows the outage probability as a function of the power allocation coefficient a_1 when the SNR is set as 30 dB. The outage probability of User 2 increases with the increase of a_1 due to interference and the decrease of its own power allocation. As a_1 increased, the outage probability of User 1, the BD, and overall first decreased and then increased. This is because User 1 first needs to decode x_2 before decoding x_1. Therefore, there is an optimal power allocation value that can minimize the outage probability of the backscatter link.

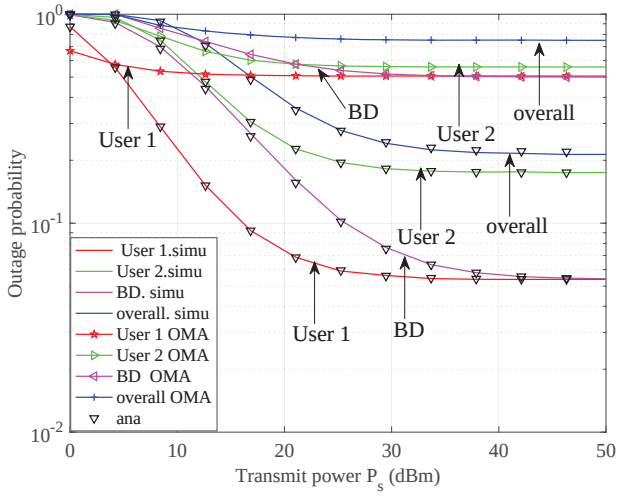

Fig. 4. The Outage performance of proposed system under different schemes NOMA and OMA.

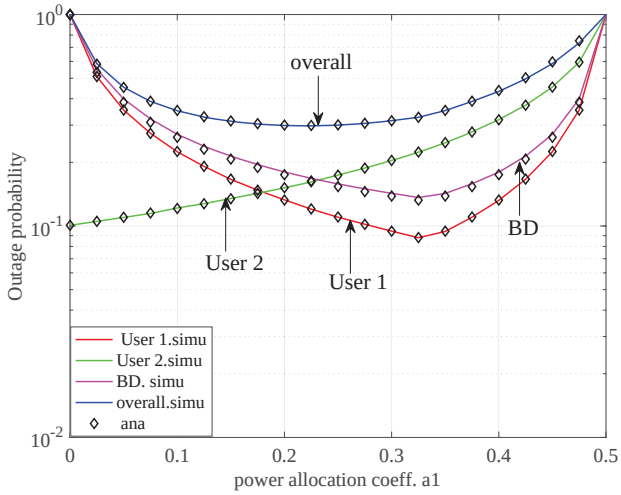

Fig. 5. The Outage performance against power allocation coeff a_1.

V. Conclusion

In this paper, we analyzed the outage performance of the backscatter-NOMA scheme. Taking into account the power consumed by the BD and employing a practical non-linear EH model, we have derived the outage probability over Rayleigh fading channels. The veracity of the analytical findings was corroborated through numerical validations. The investigation delineates the substantial impact of the BD's power consumption on the system's outage performance. If the power consumed by the BD is not considered, then the final results will overestimate performance. Moreover, the outage performance of the backscatter-NOMA scheme outperformed the OMA scheme.

REFERENCES

[1] N. Nomikos, T. Charalambous, D. Vouyioukas, G. K. Karagiannidis, and R. Wichman, "Hybrid noma/oma with buffer-aided relay selection in cooperative networks," *IEEE Journal of Selected Topics in Signal Processing*, vol. 13, no. 3, pp. 524–537, 2019.

[2] A. K. Lamba, R. Kumar, and S. Sharma, "Power allocation for downlink multiuser hybrid noma-oma systems: An auction game approach," *International Journal of Communication Systems*, vol. 33, no. 7, p. e4306, 2020.

[3] X. Yue, Y. Liu, S. Kang, A. Nallanathan, and Z. Ding, "Exploiting full/half-duplex user relaying in noma systems," *IEEE Transactions on Communications*, vol. 66, no. 2, pp. 560–575, 2017.

[4] D. Li and Y.-C. Liang, "Adaptive ambient backscatter communication systems with mrc," *IEEE Transactions on Vehicular Technology*, vol. 67, no. 12, pp. 12 352–12 357, 2018.

[5] G. Wang, F. Gao, R. Fan, and C. Tellambura, "Ambient backscatter communication systems: Detection and performance analysis," *IEEE Transactions on Communications*, vol. 64, no. 11, pp. 4836–4846, 2016.

[6] Y. Ye, L. Shi, X. Chu, and G. Lu, "On the outage performance of ambient backscatter communications," *IEEE Internet of Things Journal*, vol. 7, no. 8, pp. 7265–7278, 2020.

[7] D. Zhang and Q. Zhu, "Outage analysis for multi-bd symbiotic radio system," *IET Communications*, 2022.

[8] Y. Liu, J. Ma, Y. Ye, X. Li, and Y. Zhao, "Outage performance of backcom systems with multiple self-powered tags under channel estimation error," *IEEE Communications Letters*, vol. 26, no. 7, pp. 1548–1552, 2022.

[9] S. Zeb, Q. Abbas, S. A. Hassan, A. Mahmood, R. Mumtaz, S. M. Hassan Zaidi, S. Ali Raza Zaidi, and M. Gidlund, "Noma enhanced backscatter communication for green iot networks," in *2019 16th International Symposium on Wireless Communication Systems (ISWCS)*, 2019, pp. 640–644.

[10] Y. Liu, Y. Ye, and R. Q. Hu, "Secrecy outage probability in backscatter communication systems with tag selection," *IEEE Wireless Communications Letters*, vol. 10, no. 10, pp. 2190–2194, 2021.

[11] S. Li, Q. Li, J. Liu, and X. Cui, "Non-orthogonal multiple access in backscatter communication system under the scene of the moving reader," *Transactions on Emerging Telecommunications Technologies*, p. e4543, 2022.

[12] M. Elsayed, A. Samir, A. A. A. El-Banna, X. Li, and B. M. ElHalawany, "When noma multiplexing meets symbiotic ambient backscatter communication: Outage analysis," *IEEE Transactions on Vehicular Technology*, vol. 71, no. 1, pp. 1026–1031, 2022.

[13] Q. Zhang, L. Zhang, Y.-C. Liang, and P.-Y. Kam, "Backscatter-noma: A symbiotic system of cellular and internet-of-things networks," *IEEE Access*, vol. 7, pp. 20 000–20 013, 2019.

[14] C.-B. Le, D.-T. Do, A. Silva, W. U. Khan, W. Khalid, H. Yu, and N. D. Nguyen, "Joint design of improved spectrum and energy efficiency with backscatter noma for iot," *IEEE Access*, vol. 10, pp. 7504–7519, 2021.

[15] M. Elsayed, A. Samir, A. A. A. El-Banna, K. Rabie, X. Li, and B. M. ElHalawany, "Symbiotic ambient backscatter iot transmission over noma-enabled network," in *ICC 2022-IEEE International Conference on Communications*. IEEE, 2022, pp. 2266–2271.

[16] C.-B. Le, D.-T. Do, A. Silva, W. U. Khan, W. Khalid, H. Yu, and N. D. Nguyen, "Joint design of improved spectrum and energy efficiency with backscatter noma for iot," *IEEE Access*, vol. 10, pp. 7504–7519, 2022.

[17] H. Yang, H. Ding, M. Elkashlan, H. Li, and K. Xin, "A novel symbiotic backscatter-noma system," *IEEE Transactions on Vehicular Technology*, pp. 1–6, 2023.

Xinying Li was born in 1978, female, associate professor, master's supervisor, and teacher at the Department of Communication Engineering. Her main research direction is wireless communication.

Lijun Zhang was born in 1997, female, master student. Her research interest is Backscatter Communication.